An Adaptive Strategy for Elastic-Plastic Analysis of Structures with Cracks

Tereza Denyse de Araújo
denyse@ufc.br
Federal University of Ceará - UFC
Department of Structural Civil Engineering
60455-760 Fortaleza, CE, Brazil

Deane Roehl
droehl@rdc.puc-rio.br

Luiz Fernando Martha
lfm@tecgraf.puc-rio.br
Pontifical Catholic University of Rio de Janeiro – PUC-Rio
Department of Civil Engineering,
22453-900 Rio de Janeiro, RJ, Brazil

This work presents a methodology for self-adaptive finite element analysis of two-dimensional elastic-plastic structures. The self-adaptive process is based on an h-type refinement, with a posteriori error estimation. Two types of error estimators are available. The first is based on effective stress (Lee and Bathe, 1994) and the second is based on a ratio of plastic work (Peric et al., 1994). In the non-linear adaptive process for incremental plasticity analysis, a technique for interpolating analysis variables across distinct meshes (Lee and Bathe, 1994) is adopted. The von Mises yield criterion, with isotropic hardening, is adopted. Fracture problems are used to evaluate the performance of the adaptive process.
***Keywords**: finite elements, adaptive analysis, plasticity, cracks, error estimator*

Introduction

Structural and mechanical components are projected and constructed to remain operational during the structure's lifetime. However, preexistent flaws in the material originated from manufacture defects or external events can cause the collapse of the structure. The material type determines how a crack will propagate: if steadily until reaching a critical size (ductile crack growth), or if any propagation can mean the total ruin (creep crack growth).

The numerical method most widely employed in the analysis of fracture mechanics problems is the Finite Element Method (FEM). However, the quality of the approximate solution obtained is mesh dependent, requiring experienced analyst for the choice of a suitable mesh.

In linear fracture problems, for instance, the mesh must be refined in regions where high stress gradients occur, i.e., at crack tip. On the other hand, in non-linear fracture problems, the mesh must be refined in the regions where yielding occurs in order to capture the existing high deformation gradients. Adaptive methods are often used to ease this hard task for the analyst (Lee and Bathe, 1994; Peric et al., 1994; Araújo et al., 1997; Ladevèze et al., 1986; Gallimard et al., 1996; Zienkiewicz et al., 1990; Sandhu and Liebowitz, 1995). In a fracture problem, this adaptive method includes the following steps: finite element analysis, error estimation/indication, fracture/failure analysis, and mesh refinement.

Since adaptive concepts based on error estimators were first applied to finite-element models in the pioneer works of Babuska (Babuska and Rheinboldt, 1979), much research effort has been dedicated to the development of more efficient error estimators, which can be applied to complex problems. Most strategies developed for linear problems have been generalized for application to non linear problems.

Evaluation of the quality of the mesh is accomplished through a posteriori error estimator. Among the existing error estimators, the following can be highlighted: error estimator based on the constitutive relation of the problem (Ladevèze et al., 1986; Gallimard et al., 1996), on the energy dissipation rate (Zienkiewicz et al., 1990), on the plastic work rate (Peric et al., 1994), on the effective stress (Lee and Bathe, 1994; Sandhu and Liebowitz, 1995), and on the effective plastic strain (Sandhu and Liebowitz, 1995). In the present work, two error estimators were implemented: the first one is based on the effective stress, which is a modified version of the estimator proposed by Lee and Bathe (1994), and the second one is based on the plastic work rate, proposed by Peric et al. (1994).

The adaptive strategy is based on recursive spatial enumeration techniques, which consist of a binary tree partition for the boundary curves, whereas for mesh generation in the domain a quadtree partition is used (Paulino et al., 1999). The advantages of the meshing algorithm based on the quadtree technique are combined with the advantages of a boundary-contraction technique, which is based on the properties of the Delaunay triangulation (Araújo et al., 1997). Cracks may be introduced by the user at any position in the model. For each new crack configuration, the mesh is automatically generated.

The adaptive process begins with an initial finite element model. This model is solved incrementally. If the solution error in the model exceeds an acceptable level, the incremental analysis is interrupted for the current finite element model. The element size is derived based on the distribution of errors and the accuracy level to be achieved by the solution. A new finite element model is generated for the last successfully converged step. The solution variables (displacements, deformations, stresses, etc.) are then transferred from the previous mesh to the new one. In this work, the technique for variable mapping between different meshes presented by Lee and Bathe (1994) is adopted. The analysis is restarted for the current step with the variables of the previous step taken as initial values. The incremental analysis continues until the discretization convergence criterion is violated again. This procedure is illustrated in the diagram shown in Fig. 1.

The finite element analysis is carried out in the framework of an object-oriented finite-element program – FEMOOP (Finite Element Method: Object Oriented Program) – developed in the Civil Engineering Department at PUC-Rio (Martha et al., 1996).

Paper accepted September, 2008. Technical Editor: Marcelo Amorim Savi.

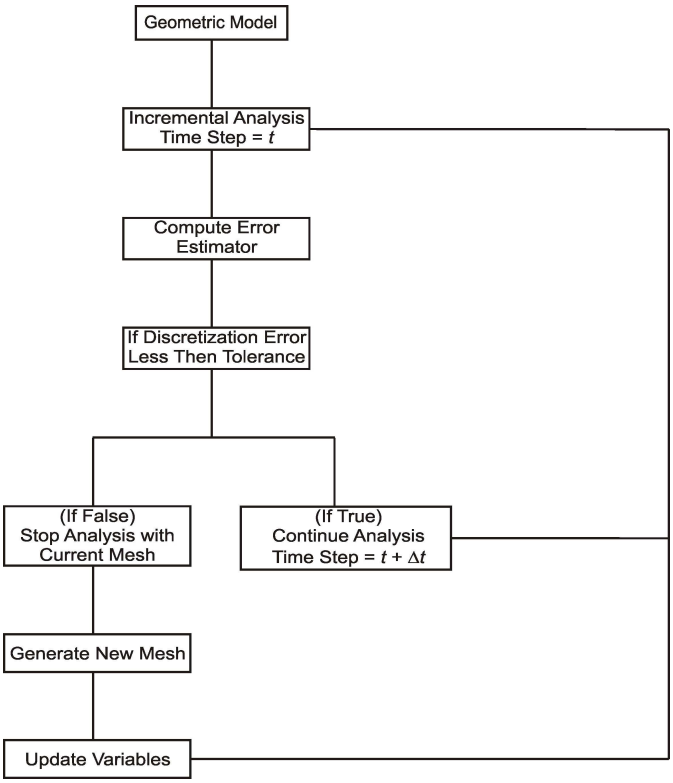

Figure 1. Diagram of the adaptive scheme for elastic-plastic analysis.

Nomenclature

A = *area integration*
a = *crack size*
C = *elastic constituive tensor; contour*
E = *elastic modulus*
e = *absolute discretization error, equivalent strain*
f = *yield criterion*
h' = *plastic modulus*
h = *size of element; half height*
J = *J integral*
K = *stress intensity factor*
N = *interpolation functions*
m = *number of elements*
n = *number of element nodes; unit outward normal*
q = *weighting function*
R = *radius*
r = *parametric coordinate*
s = *deviatoric stress, Pa; parametric coordinate*
t = *incremental time step; crack face pressure*
u = *displacement in x direction*
v = *displacement in y direction*
x = *horizontal coordinate axe*
y = *vertical coordinate axe*
W = *strain-energy density; width*

Greek Symbols

$d\lambda$ = consistency parameter
σ = stress, Pa
$\overline{\sigma}$ = effective stress, Pa
σ_Y = yielding stress, Pa
Δt = incremental time step
ε = strain, dimensionless
ζ = error ratio of element, dimensionless
Ω = relative to domain
η = relative error, (%)
$\overline{\eta}$ = admissible relative error for each element, (%)
ν = Poisson coefficient

Subscripts

E relative to generic element
ep relative to elastic-plastic
i relative to x direction
j relative to y direction
k nodal point; local crack tip axes
N new
O old
Y yielding

Superscripts

$*$ relative to smoothed, relative to preset value
e relative to elastic
h relative to discrete value
p relative to plastic, relative to the polynomial degree of the element-interpolation functions
I relative to symmetric displacement fields
II relative to anti-symmetric displacement fields

Error Estimators

In linear finite element analysis, the stresses are calculated using derivatives of the displacements. In a displacement-based FEM implementation, since no inter-element continuity for stresses is imposed, if a coarse mesh is used stress values may differ substantially between elements. This difference decreases if the mesh refinement is carried out in accordance with the order of the elements employed in the discretization. Therefore, many error estimators are based on stress discontinuities between elements (see references Zienkiewicz et al., 1990; Sandhu and Liebowitz, 1995; Li and Bettess, 1995; and Baehmann et al., 1987).

However, in elastic-plastic analysis, the constitutive model is strain driven and a better response is obtained if plastic strain discontinuity is diminished. This justifies the choice of error estimators based on plastic strains for such analysis.

Effective Stress Error

This error estimator is based on smoothed stresses, which is a global measure of the discretization error contained in a given finite element mesh. Generally this error can be expressed locally as

$$e_\sigma = \left|\sigma_{ij}^{*} - \sigma_{ij}^{h}\right| \tag{1}$$

The smoothed stresses σ_{ij}^{*} at element integration points are improved solutions for the discrete value σ_{ij}^{h} and are taken as the "exact" solution to the problem. They are obtained at element integration points with parametric coordinates, r and s, from interpolation of the nodal smoothed values $\hat{\sigma}_{ij}^{*}$ at each nodal point k.

$$\sigma_{ij}^{*} = \sum_{k=1}^{n} N_k(r,s)\left(\hat{\sigma}_{ij}^{*}\right)_k \tag{2}$$

where $N_k(r,s)$ are the interpolation functions used for the displacements and n is the number of element nodes. Here the nodal

smoothed stresses $\left(\hat{\sigma}_{ij}^{*}\right)_k$ are obtained by the super-convergent patch-recovery method (SPR) (Zienkiewicz and Zhu, 1992).

A scalar variable defined as the effective stress is introduced as

$$\bar{\sigma} = \left(\frac{3}{2} s_{ij} s_{ij}\right)^{1/2} \tag{3}$$

where s_{ij} are deviatoric stress components.

The absolute stress error in a generic element E is a direct evaluation of the error inside this element at integration points. It is expressed as

$$e_E = max\left|\bar{\sigma}^h - \bar{\sigma}^*\right| \tag{4}$$

where $\bar{\sigma}^h$ is the non-smoothed effective stress from the finite-element analysis and $\bar{\sigma}^*$ is the smoothed effective stress calculated according to Eq. (2). The absolute error in the finite element mesh corresponds to the maximum error value in the domain, i.e.,

$$e = max\left|e_E\right| \tag{5}$$

The relative error in an element is then given by the following equation:

$$\eta_E = \frac{e_E}{\left[\left(\bar{\sigma}_{max}^h\right)_\Omega^2 - \left(\bar{\sigma}_{min}^h\right)_\Omega^2\right]^{1/2}} \tag{6}$$

where $\left(\bar{\sigma}_{max}^h\right)_\Omega$ and $\left(\bar{\sigma}_{min}^h\right)_\Omega$ are the overall maximum and minimum values of $\bar{\sigma}^h$ over the domain where the error is to be evaluated. So, the value of η_E indicates the point-wise estimated relative error in effective stress.

Adaptive methods aim to achieve a uniform error distribution over the whole mesh, bringing closer the local error and the global (average) error in an iterative way during the refinement process. Then the global relative error was introduced in the strategy adopted here, which is obtained by the following expression:

$$\eta = \frac{e}{\left[\left(\bar{\sigma}_{max}^h\right)_\Omega^2 - \left(\bar{\sigma}_{min}^h\right)_\Omega^2\right]^{1/2}} \tag{7}$$

The above error estimator differs from the one presented in the work by Lee and Bathe (1994), since the latter does not consider a relative error of the mesh, as expressed in Eq. (7), but instead a local relative error for each element.

Plastic Work Error

In the presence of plastic deformations the error estimator based on the plastic work (Peric *et al*., 1994) can be expressed for an element E as

$$\left\|e_E\right\|^2 = \int_{\Omega_E} \left(\sigma_{ij}^* - \sigma_{ij}^h\right)\left[\left(\varepsilon_{ij}^p\right)^* - \left(\varepsilon_{ij}^p\right)^h\right] d\Omega_E \tag{8}$$

where $\left(\varepsilon_{ij}^p\right)^*$ and $\left(\varepsilon_{ij}^p\right)^h$ are respectively the smoothed and non-smoothed plastic strains from the finite-element analysis. The smoothed plastic strain is obtained through the same procedure described for the stresses, Eq. (2).

The relative error of the element is defined as

$$\eta_E = \frac{\left\|e_E\right\|}{\left[W^p\right]^{1/2}} \tag{9}$$

where W^p is the plastic work of the whole model calculated with the unsmoothed stresses, σ_{ij}^h, and non-smoothed plastic strains, $\left(\varepsilon_{ij}^p\right)^h$, by

$$W^p = \int_\Omega \sigma_{ij}^h \left(\varepsilon_{ij}^p\right)^h d\Omega \tag{10}$$

The global error value $\|e\|$ is given by

$$\|e\|^2 = \sum_E \left\|e_E\right\|^2 \tag{11}$$

Finally, the global relative error of the mesh, η, is obtained by:

$$\eta = \frac{\|e\|}{\left(W^p\right)^{1/2}} \tag{12}$$

Refinement Strategy

The mesh-refinement procedure is performed independently of the type of error estimator chosen. The adaptive finite element analysis is associated with a "reasonably optimal" mesh, defined as a mesh in which the specific error is uniformly distributed over the whole domain (Li and Bettess, 1995). This condition is reached by limiting the global relative error by a preset value η^*, i.e.,

$$\eta \le \eta^* \tag{13}$$

For a uniform discretization error distribution, an admissible relative error $\bar{\eta}$ for each element must be established. It is assumed that this error is the same for all mesh elements. In this case, the global relative error is given by

$$\eta = \sqrt{m\,\bar{\eta}^2} \le \eta^* \tag{14}$$

where m is the number of elements. From this relation, the admissible relative element error follows:

$$\bar{\eta} = \frac{\eta^*}{\sqrt{m}} \tag{15}$$

The new size of the element is established according to the convergence rate of the error (Li and Bettess, 1995; Zienkiewicz and Zhu, 1992), which is related to element size h, as $h \to 0$, by

$$e_E = O\left(h^p\right) \tag{16}$$

where p is the polynomial degree of the element-interpolation functions being used. With the element error given by Eq. (16) the error ratio of the element is defined by

$$\zeta_E = \frac{\eta_E}{\overline{\eta}} \tag{17}$$

for the error estimator chosen, Eq. (6) or Eq. (9). The element size ratio relates to it by

$$\frac{h_O^E}{h_N^E} = \zeta_E^{1/p} \tag{18}$$

The indexes N and O correspond to the new and to the old size of element E, respectively.

The refinement of the mesh is guided by the characteristic size of each element, which is set according to the error ratio and to the degree of the element-interpolation function. Therefore regions are refined wherever necessary ($\zeta_E > 1$), and unrefined where a coarser discretization is advisable ($\zeta_E < 1$). However, when $\zeta_E = 0$ in the adaptive plastic analysis, it means that the effective stress from the finite-element analysis is equal to the smoothed effective stress. In this case, the element size is preserved.

Mesh Adaptation

In the adaptive mesh strategy, boundary refinement is enforced independently from domain refinement. In fact, the algorithm used to refine each boundary curve is a one-dimensional version of the algorithm used to refine the domain, which is based on a quadtree technique. Each curve is decomposed by means of a binary tree technique. The idea consists of recursively subdividing the curve into segments, whereby the segment sizes are defined based on the characteristic sizes of the finite elements adjacent to the curve. At the end of this phase, after all curves of the boundary have been refined, the boundary conditions are reapplied to the model in a consistent way.

After the curves have been discretized, the new mesh is generated using the algorithm developed by Paulino et al. (1999). Details on the mesh generation scheme can be found in Araújo et al. (1997).

In the case of fracture simulation, a crack is arbitrarily introduced in the model at any phase of the analysis. A new geometry is generated and the previous mesh is deleted. A new mesh is accordingly generated keeping the same boundary discretization of the previous mesh. The same procedure carries on by crack propagation simulation. In this work examples of fixed crack configurations are described.

In a crack, both crack surfaces are considered geometrically coincident. The crack line is treated as any other geometry curve and, before the generation of the new mesh, the curve is discretized. To ensure the generation of well-shaped elements at crack tip, a standard arrangement of uniform rosette (Fig. 2) is inserted around each tip.

For elastic-plastic fracture, the rosette is composed either by quadratic triangular elements (T6) or by a special element (Barsoum, 1977) composed by a quadratic quadrilateral element degenerated into a triangle (Q8 collapsed – Q8C). In the Q8C elements the crack-tip nodes are untied and the location of the mid-side nodes is unchanged (Fig. 3). The advantage of this element is to represent the blunted plastic deformation at crack tip. It also allows crack-tip opening displacements (CTOD) to be computed from the deformed mesh.

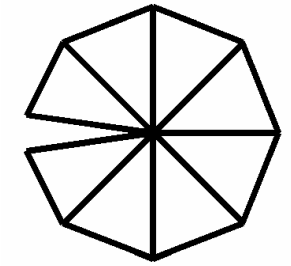

Figure 2. A standard uniform rosette.

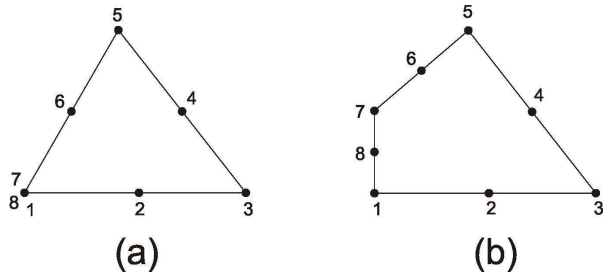

Figure 3. Q8 collapsed element: (a) Underformed element; (b) Deformed element.

Plastic State Update

Incremental description of body motion with non-linear behavior requires the establishment of the displacements and state variables at each incremental step t. In an adaptive analysis with automatic mesh generation, once a new mesh is generated, these variables must be transferred from the old mesh to the new one.

The updating process consists basically in identifying in the old mesh the element in which a node k of the new mesh is located, computing the parametric coordinates of node k in the element of the old mesh, and computing the values of the state variables at that point from element nodal values by means of interpolation using element shape functions.

To identify the element of the old mesh (E_O) that contains a node or an integration point of the new mesh, a computational-geometry algorithm (Preparata and Shamos, 1985) is employed. A straight horizontal semi-infinite line beginning at the point of interest is drawn for each element of the old mesh. If the number of intersections of the line with the element is even, the point is outside the considered element; otherwise, the point is inside it.

For crack-line curves, the search procedure described above may erroneously identify an element on an opposite face of the crack as the target element, since both faces have nodes with the same coordinates. Such nodes may belong to different elements, such as nodes at opposite crack faces, or to the same element, as happens with nodes at the crack tip for the Q8C element. Therefore, after the element is identified, an additional verification is necessary. The elements of the new and the old mesh are tested to see if they are located at the same side of the crack curve. This test is performed using an auxiliary semi-infinite control line that goes from target node k to the interior of the element E_N of the new mesh.

The incremental variables at the integration points of the old mesh are transferred to nodal values before proceeding with the mapping. This procedure can be applied to update values at both node and integration points of the new mesh.

In the present work, elastic-plastic material behavior is considered. For this material model, considering small deformations, the constitutive relations are based on the additive decomposition of the deformation tensor in its elastic and plastic components, respectively.

$$d\varepsilon_{ij} = d\varepsilon_{ij}^{e} + d\varepsilon_{ij}^{p} \tag{19}$$

In this model, the incremental stresses $d\sigma$ are related to the incremental elastic strains $d\varepsilon^e$ through the elastic constitutive tensor C:

$$d\sigma_{ij} = C_{ijkl}\, d\varepsilon_{kl}^{e} \tag{20}$$

The incremental plastic strains are defined by an associated flow rule,

$$d\varepsilon_{ij}^{p} = d\lambda \frac{\partial f}{\partial \sigma_{ij}} \tag{21}$$

in which f is the yield criterion and $d\lambda$ is a positive scalar parameter defined as the consistency parameter (Simo and Hughes, 1998). In the case that $f = 0$, the behavior is plastic and the increment of plastic strain $d\varepsilon_{ij}^{p}$ can be computed from Eq. (20), where $\partial f / \partial \sigma_{ij}$ defines the direction of the flow and $d\lambda$ defines the magnitude. In the case of $f < 0$ the increment of plastic strain is zero. These relations can be also written in the form of the well known Kuhn-Tucker complementary conditions

$$d\lambda \geq 0\,, \quad f \leq 0 \ \text{ and } \ f\,d\lambda = 0 \tag{22}$$

Isotropic hardening is considered whereby the uniaxial yield function is described through a scalar parameter identified here as the equivalent plastic strain e^p, defined for the von Mises yield as

$$\sigma_Y = \sigma_Y\left(e^{p}\right);\ de^{p} = \left[\tfrac{2}{3}\, d\varepsilon_{ij}^{p}\, d\varepsilon_{ij}^{p}\right]^{1/2} \tag{23}$$

As it can be seen from the above relations, complete description of an incremental elastic-plastic state requires, additionally to the incremental nodal displacements, the solutions for the incremental stresses, elastic and plastic deformations and the equivalent plastic strain. Due to the inter-relation of such variables, as expressed by equations (19), (20) and (23), all state variables can be obtained from the displacements at time t and the state variables at time t-Δt through numerical integration (Simo and Hughes, 1998). The plastic variables are extrapolated from the integration point to nodal points and smoothed as previously described.

J-Integral

The *J*-integral was introduced by Rice (1968) to study non-linear material behavior under small scale yielding. It is a path-independent contour integral defined as:

$$J = \lim_{C \to 0} \int_{C} \left[W n_1 - \sigma_{ij} n_j \frac{\partial u_i}{\partial x} \right] dC \tag{24}$$

where W is strain-energy density, σ_{ij} are stresses, u_i are the displacements corresponding to local i-axis, and n_j is the unit outward normal to the contour C, which is any path of vanishing radius surrounding the crack tip (Fig. 4a). The *J*-integral definition considers a balance of mechanical energy for a crack propagating along axis x.

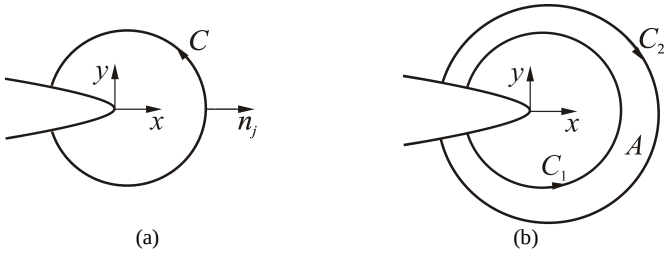

(a) (b)

Figure 4. (a) Arbitrary contour surrounding the crack tip; (b) Area to be employed to calculate the *J*-integral.

The Equivalent Domain Integral Method (Shih et al., 1986; Nikishkov and Atluri, 1987) replaces the integration along the contour with one over a finite-size domain on hand of the divergence theorem. This domain integration is more convenient for finite-element analyses. For two-dimensional problems, the contour integral is replaced by an area integral (Fig. 4b). Equation (24) is rewritten as invariant integrals, usually as defined by Knowles and Sternberg (1972):

$$J_k = -\int_A \left[W \frac{\partial \eta}{\partial x_k} - \sigma_{ij} \frac{\partial u_i}{\partial x_k} \frac{\partial \eta}{\partial x_j} \right] dA - \int_A \left[\frac{\partial W}{\partial x_k} - \sigma_{ij} \frac{\partial}{\partial x_j}\left(\frac{\partial u_i}{\partial x_k} \right) \right] q\, dA - \int_S t_i \frac{\partial u_i}{\partial x_k} q\, ds \tag{25}$$

where k is an index for local crack tip axes (x, y), q is an arbitrarily chosen continuous weighting function defined over the integration domain. A linear function was chosen for q, which assumes a unit value at crack tip and null value along the contour. In Eq. (25), t_i is the crack face pressure. For the especial case of elastic materials, the second term in this equation vanishes. These integrals were introduced initially for small deformations (Rice, 1968) and were extended by Atluri (1982) for finite deformations.

The J value is computed using the modal decomposition technique (Bui, 1983), where the displacement and stress fields are decomposed into symmetric and anti-symmetric fields with respect to the crack. The displacement field may be written as:

$$\begin{aligned} u &= u^{I} + u^{II} = \frac{1}{2}(u + u') + \frac{1}{2}(u - u') \\ v &= v^{I} + v^{II} = \frac{1}{2}(v + v') + \frac{1}{2}(v - v') \end{aligned} \tag{26}$$

where u and v are displacements in x and y directions, respectively; and $u'(x, y) = u(x,-y)$ and $v'(x, y) = v(x,-y)$. The superscripts I and II correspond to symmetric and anti-symmetric displacement fields, respectively.

The stress field may be decomposed as:

$$\begin{aligned} \sigma_{xx} &= \sigma_{xx}^{\ I} + \sigma_{xx}^{\ II} = \frac{1}{2}(\sigma_{xx} + \sigma'_{xx}) + \frac{1}{2}(\sigma_{xx} - \sigma'_{xx}) \\ \sigma_{yy} &= \sigma_{yy}^{\ I} + \sigma_{yy}^{\ II} = \frac{1}{2}(\sigma_{yy} + \sigma'_{yy}) + \frac{1}{2}(\sigma_{yy} - \sigma'_{yy}) \\ \sigma_{zz} &= \sigma_{zz}^{\ I} + \sigma_{zz}^{\ II} = \frac{1}{2}(\sigma_{zz} + \sigma'_{zz}) \\ \sigma_{xy} &= \sigma_{xy}^{\ I} + \sigma_{xy}^{\ II} = \frac{1}{2}(\sigma_{xy} - \sigma'_{xy}) + \frac{1}{2}(\sigma_{xy} + \sigma'_{xy}) \end{aligned} \tag{27}$$

where $\sigma'_{ij}(x,y) = \sigma_{ij}(x,-y)$, and $\sigma_{ZZ}^{II} = 0$.

The new integrals J_I and J_{II} have now the following properties:

$$J = J_I + J_{II} \tag{28}$$

where J_I is associated to symmetric fields (Mode I) and J_{II} is associated to anti-symmetric fields (Mode II).

In elastic-plastic analysis, the strain-energy density is divided into elastic and plastic components:

$$W = W^e + W^p \tag{29}$$

The elastic component is given by the following relation:

$$W^e = \int \sigma_{ij} d\varepsilon_{ij}^e = \frac{1}{2}\sigma_{ij}\varepsilon_{ij}^e \tag{30}$$

and the elastic-plastic component is given by Eq. (10).

The area integration in Eq. (25) is performed over an arbitrary region involving the crack tip. In this work, this region is the rosette of finite elements at crack tip. Gaussian quadrature is employed to integrate Eq. (25). Since W^p and ε_{ij}^p must be available at the nodal points, extrapolation from Gauss point values to nodal values is employed. This extrapolation is performed using a least-square fit of the Gauss point values (Hinton and Campbell, 1974).

Examples

Two examples of fracture mechanisms will now be analyzed: single-edge crack tension (Fig. 5a) and two cracks emanating from a circular hole (Fig. 5b). In these problems, the regions around the crack tips need mesh refinement because these are the places where material yielding occurs. Thus, the capability of the adaptive process to capture these regions is evaluated.

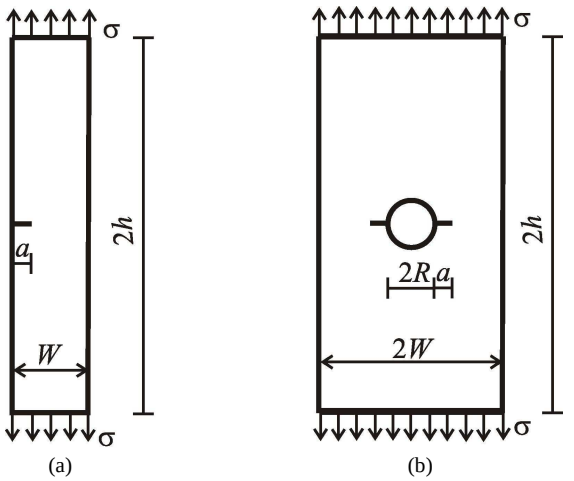

Figure 5. Elastic-plastic problem: (a) Single-edge tension crack; (b) Two cracks emanating from a circular hole.

In a previous work written by Araújo et al. (2000) a study is presented on the performance of the error estimator in effective stress (ES) and the error estimator in the plastic work rate (PW) by the elastic-plastic analysis of structures without cracks. The conclusions presented in that work point to the fact that the first estimator refines not only the yielded areas but also the areas that are still in elastic regime.

The first example presented here is analyzed using both estimators (ES and PW errors) and the second example is analyzed using the PW error estimator. The incremental analysis was carried out with the Newton-Raphson method under load control conditions.

Single-Edge Tension Crack

A plate with h/W = 2.5 and an edge crack of a/W = 0.25 is subjected to remote tensile stress σ (Fig. 5a). The following material properties are adopted: $E = 500\sigma_Y$, plastic modulus $h' = 0.05E$, and ν = 0.3 in the isotropic hardening model under plane-strain conditions.

This problem was analyzed by Nikishkov and Atluri (1994) with the finite-element method and the elastic-plastic alternating method. The finite-element model with the equivalent domain integral technique was chosen to compute the J-integral values. The results are normalized with respect to an elastic-plastic stress intensity factor $\overline{K}_{ep}$ given by

$$\overline{K}_{ep} = \frac{K_{ep}}{\sigma_Y \sqrt{\pi a}} \tag{31}$$

where K_{ep} is the elastic-plastic stress intensity factor

$$K_{ep} = \sqrt{\frac{JE}{1-\nu^2}} \tag{32}$$

In this work, this example was analyzed using both error estimators: effective stress (ES) and plastic work (PW). The two processes were carried out for both rosette types with an initial load increment of 0.1.

ES Error Estimator

A coarse initial mesh for both rosette types is given in Fig. 6a; 252 nodes were generated by the T6 rosette and 268 nodes by the Q8C rosette. The specified relative error in the effective stress η^* was set to 40% for both types of rosettes. For the Q8C rosette, the error in the initial mesh was 40.79% and occurred in the first load step (σ/σ_Y = 0.1). The incremental analysis was restarted with the new mesh (Fig. 6b), which presented a relative error of 45.34% in the third load step (σ/σ_Y = 0.3). The analysis with the second refined mesh (Fig. 6c) was restarted. Nevertheless, the error in the effective stress did not converge to the specified relative error. Adaptation of the load step did not help convergence.

When the T6 rosette was used, the relative error in the first mesh (Fig. 6a) was 43.57% for the first load step. However, when the second mesh (Fig. 7a) was analyzed, the error in the effective stress increased to 44.81% in the same step and to 58.97% in the next mesh (Fig. 7b). If a new mesh was generated for a new load increment, the error still did not converge, even for smaller increments.

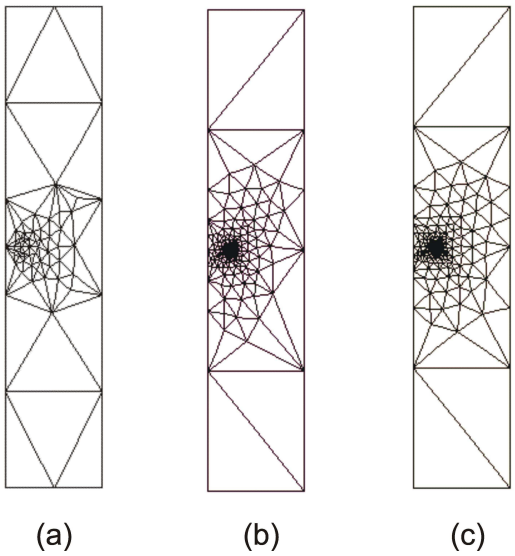

Figure 6. Adaptive process for single edge crack – ES error estimator – Q8C rosette (η^* = 40%): (a) Initial mesh – 115 elements – η = 40.79%; (b) Refined mesh 1 – 854 nodes and 401 elements – η = 45.34%; (c) Refined mesh 2 – 1625 nodes and 774 elements.

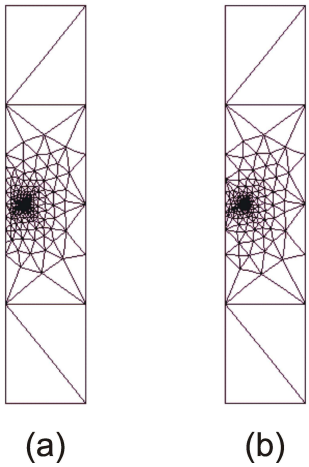

Figure 7. Adaptive process for single edge crack – ES error estimator – T6 rosette (η^* = 40%): (a) Refined mesh 1 – 1053 nodes and 506 elements – η = 44.81%; (b) Refined mesh 2 – 1604 nodes and 771 elements – η = 58.97%.

These results show that the elements around the crack tip become smaller at each adaptive step. This may be explained by the fact that these elements capture the plastic zone (Banthia, 1985). The maximum and minimum stresses inside these elements were almost the same, producing high global relative errors in effective stress – see Eq. (8). Figure 8 shows the effective stress distribution in the crack tip region. In the Q8C rosette (Fig. 8a) the stresses are non-symmetric and out of the expected range, indicating a problem in the analysis. However, in the T6 rosette (Fig. 8b) the stress distribution corresponds to small scale yielding as expected.

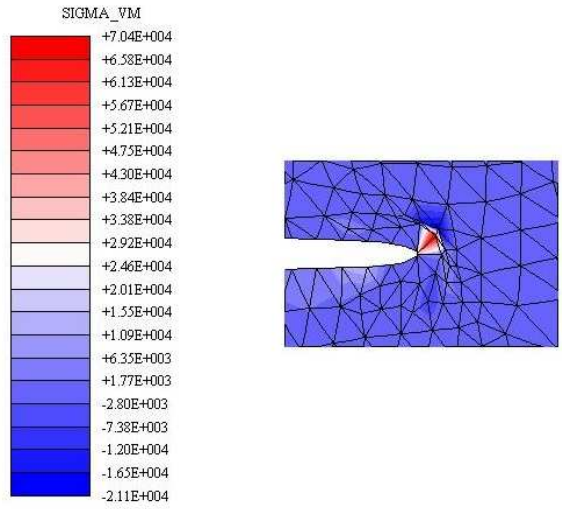

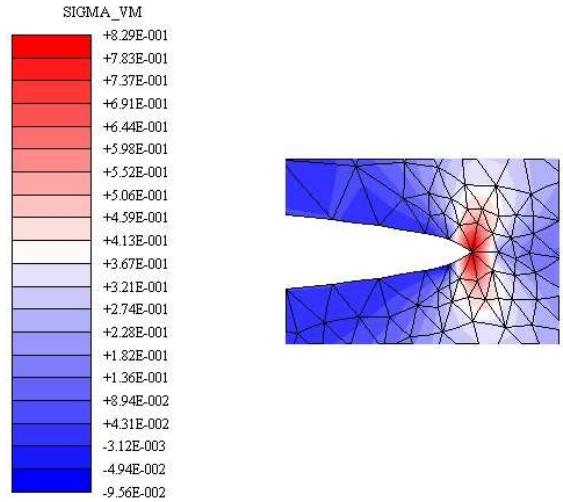

Figure 8. Effective stress distribution in the crack tip region: (a) Q8C rosette – refined mesh 2; (b) T6 rosette – refined mesh 1.

PW Error Estimator

In this case, the initial mesh was the same of Fig. 6a. The error tolerance η^* was set to 20% for T6 rosette and 45% for the Q8C rosette.

In the first case (T6 rosette), the adaptive process started by a relative error in the plastic work rate of 53.28% in the fourth load step. The incremental analysis was restarted with the new mesh of Fig. 9a. A new load increment of 0.2 was set, resulting in two steps to the end of the analysis. The error in this mesh was 2.62%. The normalized elastic-plastic stress intensity factor is shown in Figure 9b, compared to the values obtained with the initial mesh without adaptation (Araújo *et al*., 2000) and to those presented by Nikishkov and Atluri (1994).

For the Q8C rosette, the relative error in the plastic work in the initial mesh was 68.96%. It occurred in the second load increment. The incremental analysis continued with the new mesh (Fig. 10a) and with a load increment of 0.2. Five steps were necessary to accomplish the analysis. The final error was 7.71%. The results are presented in Fig. 10b.

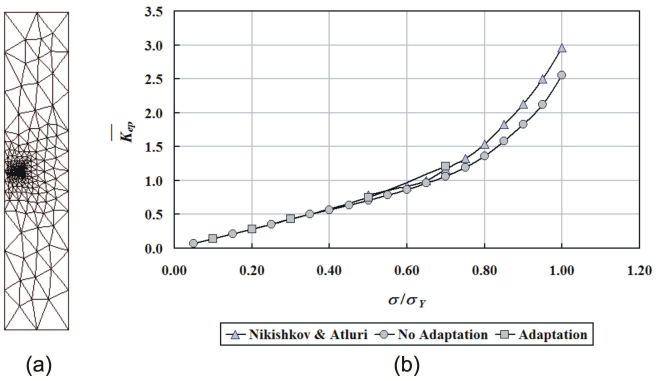

Figure 9. Adaptive process for single edge crack – PW error estimator – T6 rosette (η^* = 20%): (a) Refined mesh – 1233 nodes and 590 elements – η = 2.62%; (b) Normalized elastic-plastic stress intensity factor.

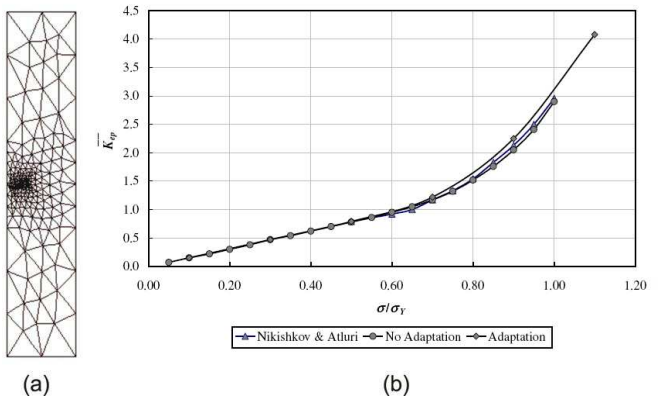

Figure 10. Adaptive process for single edge crack – PW error estimator – Q8C rosette (η^* = 45%): (a) Refined mesh – 945 nodes and 442 elements – η = 7.71%; (b) Normalized elastic-plastic stress intensity factor.

It can be noticed that, for both analyses, the results converge to the solutions presented by Nikishkov and Atluri (1994). However, the results of the initial mesh without adaptation did not converge for the T6 rosette. It may be observed that both estimators lead to reasonable meshes. The PW error estimator leads to more uniform meshes than the ES error estimator, and both refined only the region adjacent to the crack tip, as expected.

The equivalent plastic strain distributions are shown in Fig. 11. It can be noticed that, for both analysis, the distributions represent small scale yielding where the region next to crack presents plastic deformation.

Two Cracks Emanating From a Circular Hole

The second example is a plate with two symmetrical cracks emanating from a central circular hole presenting the following aspect ratios: R/W = 0.25, h/W = 2, a/R = 0.75. The material properties are the same as in the previous example. Plane-strain conditions are assumed.

This example was also analyzed by Nikishkov and Atluri (1994) considering the finite-element method. The normalized elastic-plastic stress intensity factor is given by

$$\overline{K}_{ep} = \frac{K_{ep}}{\sigma_Y \sqrt{\pi(R+a)}} \tag{33}$$

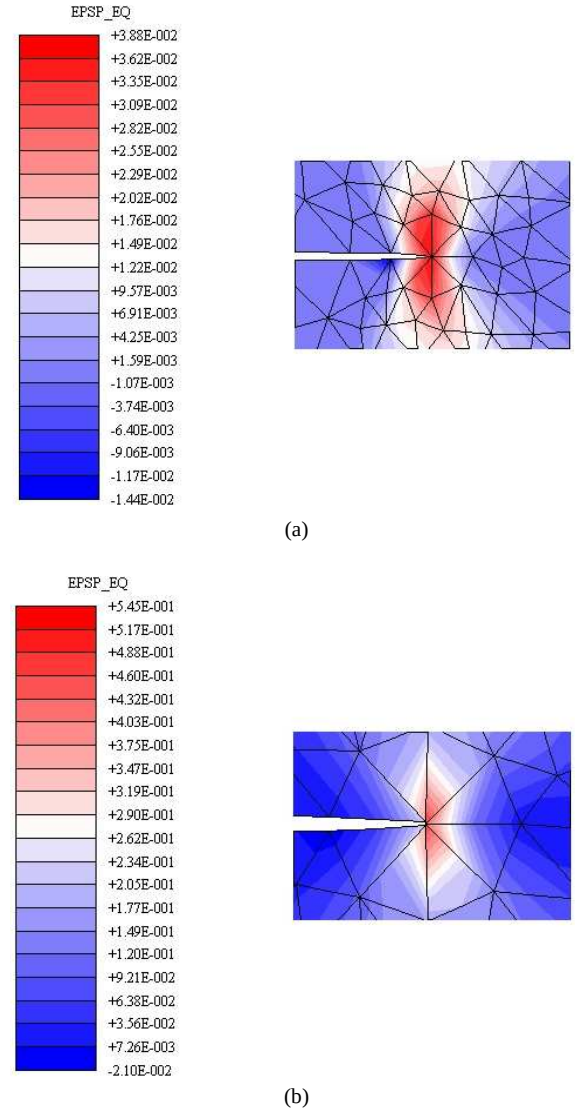

Figure 11. Equivalent plastic strain distributions in the crack tip (refined meshes): (a) T6 rosette; (b) Q8C rosette.

The two types of rosettes are also considered here. The initial mesh (Fig. 12a) presents 570 nodes by the T6 rosette and 602 nodes by the Q8C rosette, for a total of 266 elements each. The convergence criterion adopted is η^* = 30% for the first rosette and η^* = 50% for the second rosette. The initial load increment is set to σ/σ_Y = 0.1.

For the T6 rosette, the incremental analysis was interrupted at the third load step (σ/σ_Y = 0.3) with a relative error in plastic work rate of 56.5%. The new refined mesh (Fig. 12b) was analyzed considering a new load increment (σ/σ_Y = 0.2), resulting in four steps to the end of the analysis. The initial values for the analysis with the new mesh were updated from the values obtained in the second load step for the old mesh. The final error of this mesh was 4.73%. It can be seen that the refinement occurred only around the crack tip. For the Q8C rosette, the analysis of the first mesh (Fig. 12a) was interrupted in the second load step (σ/σ_Y = 0.2) with a relative error of 60.53%. The analysis continued with the second mesh (Fig. 12c) without changing the load increment. A total of 10

steps were necessary to accomplish the analysis and the final relative error was 5.50%.

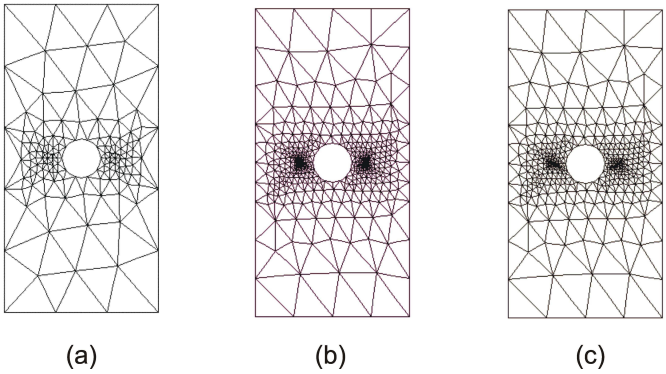

Figure 12. Adaptive process for cracks emanating from a hole: (a) Initial mesh – 266 elements; (b) Refined mesh – T6 rosette (η^* = 30%) – 2004 nodes and 966 elements – η = 4.73%; (c) Refined mesh – Q8C rosette (η^* = 50%) – 1656 nodes and 778 elements – η = 5.50%.

The *J*-integral values were compared with the solutions obtained by Nikishkov and Atluri (1994) and with the ones for the initial mesh without adaptation (Araújo et al., 2000). They are shown in Fig. 13. It is verified that all curves are coincident, i.e., the initial mesh already provides good results for the fracture parameters. However, in order to obtain the required accuracy for the plastic variables the adaptation was necessary and the plastic work estimator identified correctly the high gradient regions.

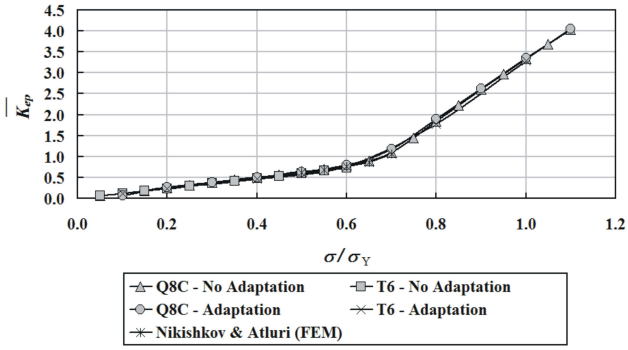

Figure 13. Normalized elastic-plastic stress intensity factor for cracks emanating from hole.

Conclusions

The main advantage of an adaptive process is the capability of starting the analysis of a model with a coarse mesh and, along the adaptive steps, automatically obtain a better final mesh, which generates results close to the 'exact values'. This goal was achieved with the proposed adaptive strategy for elastic-plastic analysis of cracked structures. The examples presented in this work show the efficiency of the proposed adaptive strategy by both refining and unrefining the model. The adaptive process efficiently located the yielding areas that are not identified *a priori*.

It is also worth pointing out that the technique used to interpolate the solution variables between the original mesh and the refined mesh has proven adequate for an elastic-plastic fracture analysis. From the presented examples, some conclusions can be drawn.

It is not advisable to use the error estimator in effective stress for the adaptive process of cracked structures. In the examples shown, when this estimator was adopted, the adaptive process at the crack tip region did not converge, independently from the type of rosette chosen. The meshes obtained with this estimator are as smoothly graded as the ones obtained with the plastic work estimators.

The value of the convergence tolerance interferes in the adaptive process mainly for the rosette composed of collapsed quadratic quadrilateral elements (Q8C rosette). When the error tolerance is low, around 5%, these elements become excessively small. However, for relatively large tolerance values, around 20%, the final discretization error after refinement reduces to low values after a small number of adaptive steps.

The *J*-integral values can diverge from the reference solutions when the Q8C rosette is used, mainly if the integration domain falls inside the plastic zone. Thus, the adaptive process for crack problems depends on the degree of mesh refinement that is specified by the convergence criterion, on the type of problem and on the initial mesh. In the examples, the T6 rosette always tends to converge to the reference solutions and should be preferred.

References

Araújo, T.D.P., Cavalcante Neto, J.B., Carvalho, M.T.M., Bittencourt, T.N., Martha, L.F., 1997, "Adaptive Simulation of Fracture Processes Based on Spatial Enumeration Techniques", *Int. J. Rock Mech. Mining Sc.*, Vol. 34:3/4, pp. 188.e1-188.e14.

Araújo, T.D., Roehl, D., Martha, L.F., 2000, "An Adaptive Strategy for Elastic-Plastic Two-Dimensional Finite Element Analysis", European Congress on Computational Methods in Applied Sciences and Engineering, Barcelona, Spain, Vol. 1, pp. 327.1-327.17.

Atluri, S.N., 1982, "Path-Independent Integrals in Finite Elasticity and Inelasticity, with Body Forces, Inertia, and Arbitrary Crack-Face Conditions", *Eng. Frac. Mech.*, Vol. 16, pp. 341-364.

Babuska, I., Rheinboldt, W.C., 1979, "On the Reliability and Optimality of the Finite Element Method", *Computer & Structures*, Vol. 10, pp. 87-94.

Baehmann, P.L., Wittchen, S.L., Sheppard, M.S., *et al*., 1987, "Robust Geometrically Based, Automatic Two-Dimensional Mesh Generation", *Int. J. Num. Meth. Eng*., Vol. 24, pp. 1043-1078.

Banthia, V., 1985, "Singularity of Collapsed Q-8 Finite Element", *Int. J. Num. Meth. Eng.*, Vol. 21, pp. 959-965.

Barsoum, R.S., 1977, "Triangular Quarter-Point Elements as Elastic and Perfectly-Plastic Crack Tip Elements", *Int. J. Num. Meth. Eng*., Vol. 11, pp. 95-98.

Bui, H.D., 1983, "Associated path independent J-integrals for separating mixed modes", *J. Mech. & Physics Solids*, Vol. 31, pp. 439-448.

Gallimard, L., Ladevèze, P., Pelle, J.P., 1996, "Error Estimation and Adaptivity in Elastoplasticity", *Int. J. Num. Meth. Eng*., Vol. 39, pp. 189-217.

Hinton, E., Campbell, J.S., 1974, "Local and Global Smoothing of Discontinuous Finite Element Functions Using Least Squares Method", *Int. J. Num. Meth. Eng*., Vol. 8, pp. 461-480.

Knowles, J.K., Sternberg, E., 1972, "On a Class of Conservation Laws in Linearized and Finite Elastostatics", *Archives for Rational Mechanics & Analysis*, Vol. 44, pp. 187-211.

Ladevèze, P., Coffignal, G., Pelle, J.P., 1986, "Accuracy of Elastoplasticity and Dynamic Analysis. Accuracy Estimates and Adaptive Refinements in Finite Element Computations", pp. 181-203.

Lee, N.S., Bathe, K.J., 1994, "Error Indicators and Adaptive Remeshing in Large Deformation Finite Element Analysis", *Fin. Elem. An. & Des.*, Vol. 16, pp. 99-139.

Li, L-Y, Bettess, P., 1995, "Notes on Mesh Optimal Criteria in Adaptive Finite Element Computations", *Com. Num. Meth. Eng.*, vol. 11, pp. 911-915.

Martha, L.F., Menezes, I.F.M., Lages, E.N., Parente Jr., E., Pitangueira, R.L.S., 1996, "An OOP Class Organization for Materially Nonlinear Finite Element Analysis", Join Conference of Italian Group of Computational Mechanics and Ibero-Latin American Association of Computational Methods in Engineering Padua, Italy, pp. 229-232.

Nikishkov, G.P., Atluri, S.N., 1987, "Calculation of Fracture Mechanics Parameters for an Arbitrary Three-Dimensional Crack, by the 'Equivalent Domain Integral' Method", *Int. J. Num. Meth. Eng*., Vol. 24, pp. 1801-1821.

Nikishkov, G.P., Atluri, S.N., 1994, "An analytical-numerical alternating method for elastic-plastic analysis of cracks", *Computational Mechanics*, Vol. 13, pp. 427-442.

Paulino, G.H., Menezes, I.F.M., Cavalcante Neto, J.B., Martha, L.F., 1999, "A Methodology for Adaptive Finite Element Analysis: Towards an Integrated Computational Environment", *Comp. Mech.*, Vol. 5/6, pp. 361-388.

Peric, D., Yu, J., Owen, D.R., 1994, "On Error Estimates and Adaptivity in Elastoplastic Solid: Applications to the Numerical Simulation of Strain Localization in Classical and Cosserat Continua", *Int. J. Num. Meth. Eng*., Vol. 37, pp. 1351-1379.

Preparata, F.P., Shamos, M.I., 1985, "Computational Geometry: an Introduction", New York: Springer-Verlag.

Rice, J.R., 1968, "A Path Independent Integral and the Approximate Analysis of Strain Concentration by Notches and Cracks", *J. App. Mech.*, Vol. 35, pp. 379-386.

Sandhu, J.S., Liebowitz, H., 1995, "Examples of Adaptive FEA in Plasticity", *Eng. Frac. Mech.*, Vol. 50, pp. 947-956.

Simo, J.C., Hughes, T.J.R., 1998, "Computational Inelasticity", Springer Verlag.

Shih, C.F., Moran, B., Nakamura, T., 1986, "Energy Release Rate Along a Three-Dimensional Crack Front in a Thermally Stressed Body", *Int. J. Frac*., Vol. 30, pp. 79-102.

Zienkiewicz, O.C., Huang, G.C., Lin, Y.C., 1990, "Adaptive FEM Computation of Forming Processes – Application to Porous and Non-Porous Materials", *Int. J. Num. Meth. Eng*., Vol. 30, pp. 1527-1553.

Zienkiewicz, O.C., Zhu, J.Z., 1992, "The Superconvergent Patch Recovery and a Posteriori Error Estimates. Part 1. The Recovery Technique", *Int. J. Num. Meth. Eng*., Vol. 33, pp. 1331-1364.